International Journal of Science Academic Research
Vol. 01, Issue 08, pp.518-522, November, 2020
Available online at http://www.scienceijsar.com

ISSN: 2582-6425

Research Article

UNIDIRECTIONAL REFLECTIVITY IN NON-HERMITIAN LOSSY THIN FILMS

[1, 2, *] Alejandro Padrón-Godínez and [2]CarlosGerardo Treviño-Palacios

[1]Instituto de Ciencias Aplicadas y Tecnología, Universidad Nacional Autónoma de México, Circuito Exterior S/N, Coyoacán, C.P. 04510, Ciudad Universitaria - México
[2]Instituto Nacional de Astrofísica, Óptica y Electrónica, Calle: Luis Enrique Erro No. 1, Santa María Tonantzintla, C.P. 72840, Puebla – México

Received 11th September 2020; **Accepted** 15th October 2020; **Published online** 16th November 2020

Abstract

Inspired by non-Hermitian systems, we study reflection and transmission in a stack of thin films composed by the repetition of a bipartite unit cell. We aim for controlled reflection and transmission using lossless and lossy materials. In particular, we show unidirectional reflection using transfer matrix methods and confirm our results by finite element simulation.

Keywords: Thin films, PT-Symmetric, Non-Hermitian systems, Transfer matrix, Unireflectivity.

INTRODUCTION

Thin films are a standard option to design optical devices with controlled reflection and transmission. Optics has a long tradition of studying how the basic properties of materials can be used to engineer thin film structures with an overall different behavior, which might be used for industrial applications such as optical camouflage and optical rectifiers, isolators or switch to mention a few (Knittl, 1976; Feng *et al.,* 2013; Ramezani and Kottos, 2010). Recently, the quantum idea of parity time-symmetry has been used to create composite structures with interesting optical properties. PT-Symmetry in quantum mechanics refers to invariance to spatial and temporal reflection. This is provided by complex potentials that obey the property V(x) = V*(-x) (Bender and Boettcher, 1998; Lin *et al.,* 2011; El-Ganainy *et al.,* 2019). An ideal optical equivalence is to introduce linear media with equal real part of the refractive index and imaginary parts that are the complex conjugate of each other (Kottos and Aceves, 2016). Such media is practically inexistent in nature and hard to engineer but experimental realizations have shown its feasibility (Feng *et al.,* 2013). Furthermore, it has been shown that unidirectional reflection arises from PT-symmetric structures due to the gain-loss balance in optical structures that bring to mind a stack of thin film (Longhi, 2010). Here, we are interested in the effect of using real-world materials to design unidirectional reflection less stacks of thin films, Figure (1).

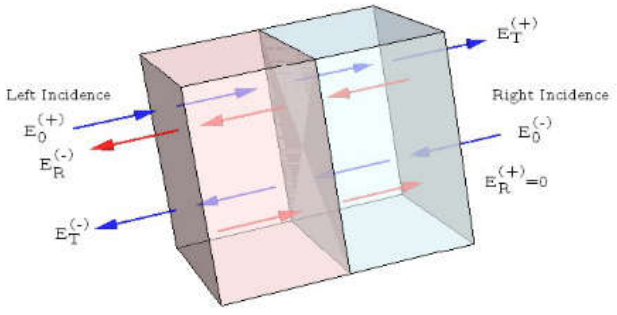

Fig. 1. A unit cell showing unidirectional reflectivity usingtwo thin films with conjugate

Corresponding Author:** ***Alejandro Padrón-Godínez
Instituto de Ciencias Aplicadas y Tecnología, Universidad Nacional Autónoma de México, Circuito Exterior S/N, Coyoacán, C.P. 04510, Ciudad Universitaria – México.

First, we are going to model electromagnetic field propagation through dielectric thin films considering left and right normal incidences. We will start with the treatment of a simple layer using multiple beam interference techniques. Then we will provide their transfer matrices and use them to describe a unit cell composed of just two thin layers [8]. Next, we will optimize the film thicknesses numerically to end the extreme values for reflectivity/transmitivity at the desired wavelength. Then, we will find the transfer matrix results for these optimized parameter values and compare them with finite element simulation. We will use the ideal gain-loss bilayer as benchmark for more realistic passive-loss values of doped silicon dioxide (SiO_2). Finally, we will show results for unidirectional reflectivity for a stack composed by three unit cells.

Transfer matrix formalism

We start our study with the treatment of a single thinlayer using style multi-beam interferometry. We consider incidence from left to right, Figure (2).

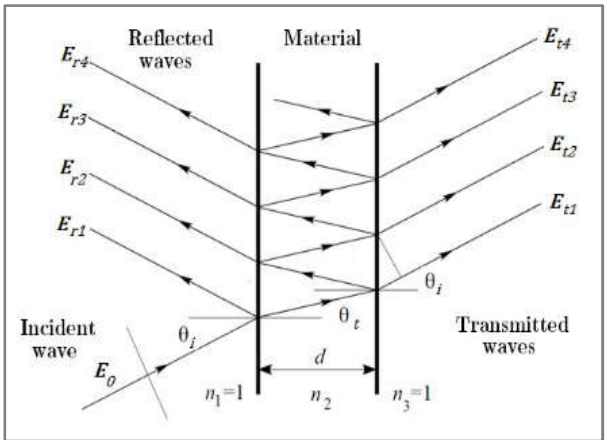

Fig. 2. Multiple reflection and transmition waves propagation in one layer

The total effective reflectivity from the left to the right boundary (Ramezani and Kottos, 2010). Forseveral reflections and transmissions:

$$t_{13} = \frac{t_{12}t_{23}\, e^{-i\phi}}{1 - r_{21}r_{23}\, e^{-i2\phi}}; \quad (1)$$

$$r_{13} = r_{12} + \frac{t_{12}t_{21}\, r_{23} e^{-i2\phi}}{1 - r_{21}r_{23}\, e^{-i2\phi}}; \quad (2)$$

Where t_{ij} and r_{ij}, are the transmissions an reflections coefficients at each boundary, with i≠ j. We will show results for normal incidence for the sake of space. The effective transfer matrix (Longhi, 2010), also called scattering matrix is given by

$$M_{net} = M_{23}\square M_{22}\square M_{12} = \begin{pmatrix} t_{23}t_{32} - r_{23}r_{32} & r_{32} \\ -r_{23} & 1 \end{pmatrix} \cdot \begin{pmatrix} e^{ik_2n_2d_2} & 0 \\ 0 & e^{-ik_2n_2d_2} \end{pmatrix} \cdot \begin{pmatrix} t_{12}t_{21} - r_{12}r_{21} & r_{21} \\ -r_{12} & 1 \end{pmatrix}, \quad (3)$$

$$S_e = \frac{1}{m_{22}} \begin{pmatrix} Det(M_{net}) & m_{12} \\ -m_{21} & 1 \end{pmatrix} = \begin{pmatrix} t_{13} & r_{31} \\ r_{13} & t_{31} \end{pmatrix} = \begin{pmatrix} \frac{t_{12}t_{23}e^{ik_2n_2d_2}}{1 - r_{21}r_{23}e^{i2k_2n_2d_2}} & r_{21} + \frac{t_{32}r_{32}t_{21}e^{ik_2n_2d_2}}{1 - r_{23}r_{21}e^{ik_2n_2d_2}} \\ r_{12} + \frac{t_{12}t_{23}r_{23}e^{ik_2n_2d_2}}{1 - r_{21}r_{23}e^{ik_2n_2d_2}} & \frac{t_{32}t_{21}e^{ik_2n_2d_2}}{1 - r_{23}r_{21}e^{i2k_2n_2d_2}} \end{pmatrix}, \quad (4)$$

where k_2 is the wave number in the material, d_2 is the width of layer thin, n_2 is the refraction index, t_{13} and $r_{13}$are the transmission and reflection coefficients for left side incidence then r_{31} and $t_{31}$are the reflection and transmission coefficients considering right side incidence. When we have a layer with complex refractive index, $n_{ci} = n_i + ik_i$,a negative imaginary part, $k_i < 0$, provides gain and loss is obtained with $k_i > 0$. In addition, transmission and reflection for a field impinging on the left side are given byt_{13} and r_{13} and for a right impinging field r_{31} and t_{31}. We will use the same method when we will have a stack of unit cells as Figure (3).

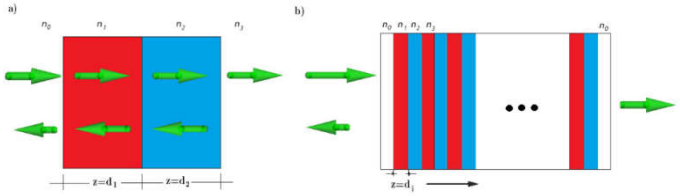

Fig. 3. a) Unit cell N=1. b) Stack of unit cells N=1, 2, 3,...

Semiconductor and Thin Films

The basic material used in the construction of most diodes and transistors is Silicon (Si), silicon is a semiconductor at room temperature very few electrons exist in the conduction band of the silicon crystal. When a proportional current is applied to a group of moving electrons, the current is small, the material has great resistance. The conduction and valence bands of pure silicon are shown in Figure (4).

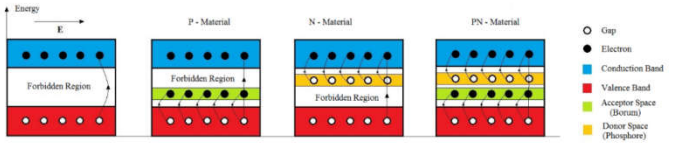

Fig. 4. The conduction and valence bands of pure Silicon

At 0[K] (absolute zero), all electrons are at their lowest energy level, at room temperature occasionally an electron has a lot of energy to escape the valence band and move towards the conduction band. The lack of electrons is shown as a circle or hole, if an electric field is applied to the material the electron moves towards the positive terminal of the battery. An electron in the valence band can also move towards the positive terminal of the battery if it has enough energy to go from its energy level to the energy level of the hole. When this electron escapes from a gap, it leaves it hidden. The gaps would appear to be moving to the right, towards the negative battery terminal. The current network is therefore the sum of the current due to the movement of the electrons in the conduction band and of the current due to the movement of the gaps in the valence band (Schilling and Belove, 1989). The conventional current due to the flow of electrons and the current of gaps are in the direction of the electric field.

Thin Films

Similarly, the use and procedure we make for the construction of an electric diode is used to create thin films that will serve to create an optical diode in this case and to carry out on this device the study and analysis when electromagnetic radiation is applied by two normal directions opposite. In thin films we look first to have symmetry-PT, after doping with other materials. Which we accomplish with a pair of semiconductor dielectric (dimer) layers with balanced gain and loss. However, to achieve a symmetry of the device we must optimize its thickness using parameters on which we want to obtain the results, such as wavelength, complex refractive indices, to name a few. Using thin film layers, we can use various combinations of passive-doping as gain-gain in the dimer, or loss-loss, up to layers such as gain-loss, real-loss, real-gain (Poladian, 1996).

Design and construction of study materials

For the analysis of this work, we look for materials based on semiconducting dielectric thin films, which have a behavior similar to that of a signal rectifier diode. The basis of these materials were originally thin layers of Silicon and Germanium. The material studied starts from SiO2 that has the following properties when thin films are deposited on a substrate with refractive index n_r = 1.4574, anextinction coefficient κ = 0.000687, at a wavelength of 1510 [nm], (Rodríguez-de Marcos *et al.,* 2016).

This material is constructed by means of a reactive electron beam, evaporated on various substrates at 300 [°C], as is done in the manufacture of CMOS transistors (Hodgson and Olsen, 2003). We build a first material similar to that shown in Figure (4d), which has an acceptor and donor in the valence bands as a rectifier diode that is polarized in direct current (Padrón-Godínez *et al.,* 2019). Generating a PN-material with Boron and Phosphorus, which corresponds to a material with balanced gain and loss based on a pair of thin films, known as a dimer with parity time symmetry (PT).We also require a second material constructed with acceptor valence bands like the one in Figure (4b), doped with Boron as an N-material. Thus creating a pure material in its first layer and with absorption in the second layer, which corresponds to a dimer with a passive layer and a layer with loss. These materials that have been tested at the electrical system level, we now study them to create optical rectifiers that are important in the construction of entangled photon generating stable sources (Padrón-Godínez *et al.,* 2020). The properties of these dimers

based on doped SiO_2 dielectric thin films have dielectric constants equal to

$$\varepsilon = \varepsilon_0 \pm i\,\varepsilon_i\,, \tag{5}$$

Where ε_0 = 2.3963 and ε_i = 0.3003. So we will use for a balanced dimer $\varepsilon = \varepsilon_0 - i\varepsilon_i$ in the first layer and $\varepsilon = \varepsilon_0 + i\varepsilon_i$in the second layer, gain-loss. Then for a passive dimer with loss we have $\varepsilon=\varepsilon_0$in the first layer and $\varepsilon=\varepsilon_0+ i\varepsilon_i$for the second layer, real-loss (Shramkova and Tsironis, 2016). Then we change these values to refractive index and extinction coefficient respectively (n_i=1.548, κ_i=0.548).

Optimization of thin films

We are looking for unidirectional reflection less, that is a reflection that is null in one direction but not the other (Shramkova and Tsironis, 2016; Yang *et al.,* 2016; Poladian, 1996; Novitsky *et al.,* 2019). For fixed refractive indices and impinging wavelength, we can optimize the dimer thickness for reflection or transmission using the first and second numerical derivatives of their transfer matrices.

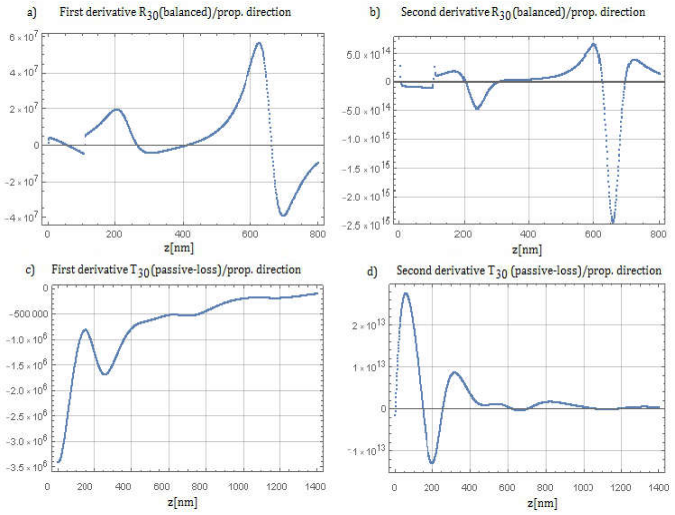

Fig. 5. a), c) First and b), d) second numerical derivate, ofthe reflection and transmission coefficients for a), b) one gain-loss and c),d) one passive-loss unit cell with normal incidence

Figure (5) shows numerical derivatives for the reflection coefficients R_{30} of a double-layer cell with balanced gain-loss and one double-layer cell with passive-loss materials at λ_r = 1550 [nm] and normal incidence, θ_i = 0. The parameters used for the ideal cell were $n_1 = n_2$ = 1.548, of silicon dioxide (SiO_2), $\kappa_1 = \kappa_2 = \pm 0.548$, and for the passive-loss cell $n_1 = n_2$ = 1.548, κ_1 = 0, κ_2 = 0.548, in both cases $n_0 = n_3$ = 1. The thickness of the layers are equal, $d_1 = d_2 = d$. We take the zeros of the first derivative that yield positive values of second derivative to find the layer thickness that yields reflectivity minima. When the electromagnetic waves propagate within a dielectric medium, the phases ϕ are cumulative and depend on the refractive index n_{ci}, the wave number k_0 and the width of the layer that in turn it depends on the wave length $d_i(\lambda_r)$. For example, the optimized thickness for reflectivity minima $R_{30}$for the balanced bilayer are d=240[nm] and d=660[nm] at the desired resonance wavelength of 1550[nm]. The optimized thickness for transmission minima $T_{30}$for passive-lossy cell are the d=200[nm] and d=660[nm] at the same desired resonance wavelength. In the following, we will simulate the propagation of linearly polarized electromagnetic field using these optimized thicknesses and compare our numerical results with finite element simulation to good agreement.

RESULTS

The system with which we start, as in equation (3) for the case of two layers is the transfer matrix now given by

$$M_{net} = M_{23}\square M_{22}\square M_{12}\square M_{11}\square M_{01}\,, \tag{6}$$

with it we get the effective dispersion matrix, in terms of the reflection and transmission coefficients

$$S_e = \frac{1}{m_{22}}\begin{pmatrix} Det(M_{net}) & m_{12} \\ -m_{21} & 1 \end{pmatrix} = \begin{pmatrix} t_{03} & r_{30} \\ r_{03} & t_{30} \end{pmatrix}, \tag{7}$$

that we can express it as the system of equations to analyze the propagation in the direction of the z-axis to a quarter of the resonance wavelength

$$\begin{pmatrix} E_3^{(+)} \\ E_0^{(-)} \end{pmatrix} = \frac{\lambda_r}{4n_e} S_e \begin{pmatrix} E_0^{(+)} \\ E_3^{(-)} \end{pmatrix}. \tag{8}$$

From the effective scattering matrix, the analysis of the eigenvalues is performed for one quarter of the wavelength propagation. This analysis is similar to the autonomous treatment of a system of ordinary second-order differential equations of the form

$$\frac{dE_3^+}{dz} = f(r,t), \qquad \frac{dE_0^-}{dz} = \; g(r,t). \tag{9}$$

For the roll that is being analyzed, the effective scattering dispersion matrix contains reflectivity and transmitivity based on complex refractive indexes. As presented the loss or gain extinction coefficient κ_i respectively is the parameter that can balance the optical device based on thin dielectric films for photon entanglement source. Therefore, the trajectories of the eigenvalues of the effective scattering matrix are presented below. To illustrate the PT-Symmetry in the figure (6b and 6e) the eigenvalues λ_1 y $\lambda_2$with reals and imaginary parts, show reals values of $1 \le (\lambda_1,\lambda_2)$ from $\kappa_2 = -0.548$ and $0 \le (\lambda_1,\lambda_2)$in the range $-0.548 \le \kappa_2 \le 0.548$in the imaginary part of$(\lambda_1,\lambda_2)$.

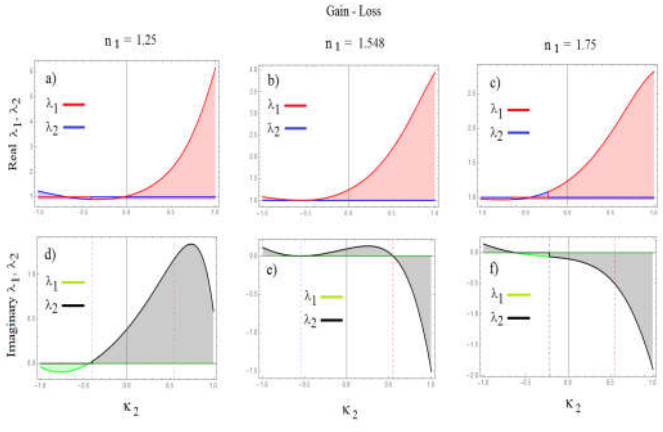

Fig. 6. Eigenvaluesλ_1, $\lambda_2$versusextinction coefficientκ_2 gain-loss, reals a), b) and c);imaginaries d), e) y f).

When you change the value of n_1 = 1.25 the symmetry is broken in κ_2 = -0.4, with1≤ (λ_1,λ_2) for reals and 0 ≤ (λ_1,λ_2) for imaginaries, Figure (6a and 6d). When the value of the refractive index of the first layer changes to n_1 = 1.75 the symmetry is broken in κ_2 = -0.22, with1≤ (λ_1,λ_2) for reals and 0 ≥ (λ_1,λ_2) for imaginaries, figure(6c y 6f). In the case of losing thin films, a real-loss dimer is found with n_{c1} = 1.548 in the first layer and n_{c2} = $n_{2\pm}$i κ_2 in the second layer, $\kappa_2$varies between [-0.75, 0.75] for a value of $z_1 = z_2 = \lambda_r/4n_{cj}$, with j = 1, 2. Among the paths of linear system solutions, equation (8), these can be described depending on the determinant of the matrix. For example, if the determinant is zero or nonzero, or the matrix trace is proportional to the matrix determinant. For the effective scattering matrix of a real-loss dimer you have to

$$tr\,|S_e| = \frac{1}{4}\det|S_e|, \tag{10}$$

Therefore it is a parabolic moved in the vertical, that is, it has a certain shape that will be shown in the solutions. To illustrate the dynamics of passive-loss dimer, it has the Figure (7b), showing the graphs of the reals and imaginary eigenvaluesλ_1 and λ_2 versus gain–loss extinction coefficient in an interval of-0.75≤κ_2≤0.75. In the case of passive dimer with loss the curve solution is a parabolic for λ_1 and for λ_2 is kept constant at 1 depending on the change of $\kappa_2$between [-0.75, 0.75].For imaginary λ_1 the solution curve is a logistics with stable node at (0,0) and for imaginary λ_2 remains constant at 0 in the same range of κ_2. This is shown in figure (7b and7e).

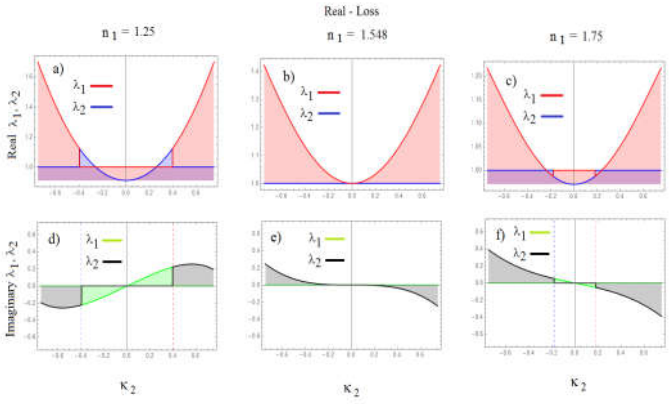

Figure 7. Eigenvalues λ_1, λ_2 versus extinction coefficientκ_2 gain-loss, reals a), b) y c);imaginaries d), e) y f).

In the event that the value of n_1 = 1.25 is changed, the symmetry is broken inκ_2=± 0.4, the parabolic moves vertically downwards with real and imaginary values out of the string,(λ_1,λ_2), figure (7a and7d). When the refractive index value of the first layer changes to n_1 = 1.75 the symmetry is broken in κ_2= ±0.18, equally the parabolic path moves down with real and imaginary values within the curve, Figure (7c and7f).Now we show the dynamics of the reflectivity and transmitivity of the thin film arrangements in studio. The ideal dimer balanced with PT-Symmetry and the passive dimer with real-loss, Figure (8) shows the reflectivity and transmitivity for some periodic structures.

Figure (8a) shows these values for an optimized bilayer thickness of d =240[nm] where we can see that reflectivity from the left side, R_L, dominates over that from the rightside, R_R, atλ_r = 1550[nm], which is showed as a vertical line. Similarly, figure (8d) shows reflectivity and transmitivity values for an optimized bilayer thickness of d = 660[nm]. If we wanted to use this bilayer and repeat it as unit cell in astack, say N = 3, and 5, the wavelength showing a maximum difference in reflection will shift. Thus, we have to optimize for each and every stack size to recover similar results to the N = 1 and N=3 case, figure (8b and 8e). Then we can again see that reflectivity from the left-side dominates over that from the right-side. Now, a wavelength shift occurs if we increase the number of unit cells N=5 without further optimization, figure (8c and 8f). In order to see difference between optimized and non-optimized stack.

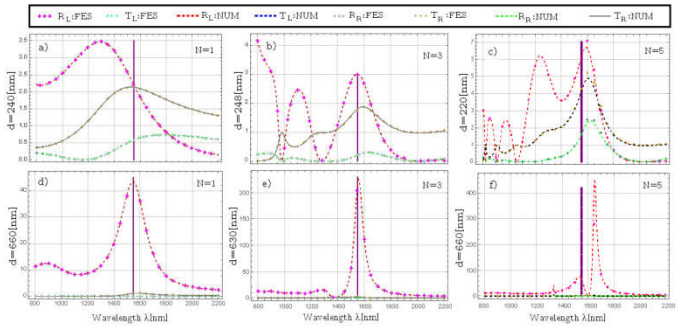

Fig. 8. Reflectivity and transmitivity in an ideal balanced double-layer, Numeric (NUM) and finite element simulation (FES)

Now, we move into a more realistic passive-loss structure, namely real-loss dimer. Furthermore, Figure (9) shows the reflectivity and transmitivity for passive-loss structures. Figure (9a and 9d) shows the reflectivity and transmitivity values for an optimized bilayer thickness of d = 150[nm] and d=200[nm] respectively. Where now, we can see that reflectivity from the right R_R dominates over that from the left R_L at λ_r = 1550[nm] (vertical line).

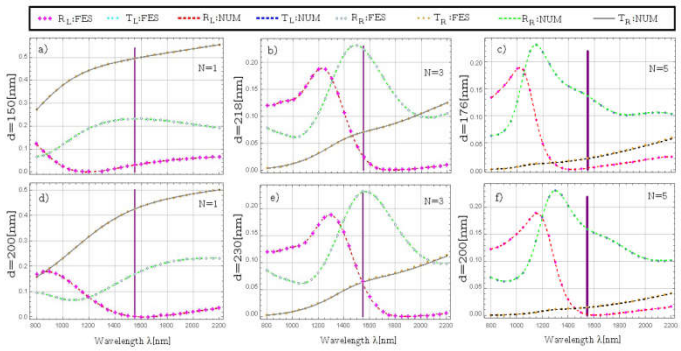

Fig. 9. Reflectivity and transmitivity in a passive-loss double-layer cell, Numeric (NUM) and finite element simulation (FES)

In a stack of N=3, we see the same behavior the reflectivity R_R dominates over that from the left R_L. Here we have a coincidence between R_L and Transmitivity both side (T_L=T_R) in λ_r, when is d=230[nm] of each thin film, Fig. (9c and 9f). When we have a stack of non-optimized N=5 unit cell a wavelength shift is induced, Fig. (9c and 9f). In addition, here is only to see optimized stacks differences.

DISCUSSION

Many studies of non-Hermitian systems may have advantages in the construction of new materials for the field of nonlinear optics. In the literature, we have found non-Hermitian

processes for the generation of coherent light sources with the mixture of waves without phase coincidence restrictions as in the case of entangled photons and the conservation of momentum, which represents a need for the creation of efficient radiation in standard nonlinear optics.

Conclusion

We have shown that optimization of thin film structures, using transfer matrix analysis; can yield optimal parameters for structures with bidirectional transmission but unidirectional reflection. We presented two cases for two different optimal values of thin film thickness. One being the bipartite unit cell with balanced gain-loss and the other a passive-loss structures. Finally, we want to stress that the width of the unit cell must be optimized for the desired stack size; otherwise, unidirectional reflectivity will occurat a different wavelength. Of course, in the more realistic passive-loss unit cell, the transmitivity will decrease with the size of the stack as a result of the losses.

Acknowledgements: This work has been sponsored by "Dirección General deAsuntos del Personal Académico de la Universidad Nacional Autónoma de México" under the "Programa de Apoyospara la Superación del Personal Académico (PASPA)" through doctoral scholarship. The author thanks B. M. Rodríguez-Lara for fruitful discussion.

Authors contributions: All the authors were involved in the preparation of the manuscript. All the authors have read and approved the final manuscript.

Disclosures: The authors declare no conflicts of interest.

REFERENCES

Bender, C. M., Boettcher, S. 1998. "PT-symmetric quantum mechanics". Phys. Rev. Lett. 80, 5243, https://doi.org/ 10.1103/ PhysRevLett.80.5243

El-Ganainy, R., Khajavikhan, M., Christodoulides, D. N., Ozdemir, S. K. 2019. "The dawn of non-Hermitian optics". Communications Physics. 2:37, https://doi.org/10.1038/ s42005-019-0130-z | www.nature.com/commsphys.

Feng, L., Xu Y.L., Fegadolli W. S., Lu M., Oliveira J.,Almeida V. R., Chen Y., Scherer A. 2013. "Experimental demonstration of a unidirectional reflectionless PT metamaterial at optical frequencies". Nat. Mat. 12, 108-113. DOI:10.1038/NMAT3495.

Hodgson, D., Olsen, B. 2003."Protecting Your Laser Diode", ILX Light wave Corporation.

Knittl, Z. 1976. "Optics of Thin Films", Ed. John Wiley and Sons.

Kottos, T., Aceves, A. B. 2016. "Contemporary Optoelectronics". Springer Series in Optical Sciences 199. DOI:10:1007=978 / 94 / 017 / 7315 / 7 / 9

Lin, Z., Ramezani H., Eichelkraut, T., Kottos, T., Cao, H., Christodoulides, D. N. 2011. "UnidirectionalInvisibility Induced by PT-Symmetric Periodic Structures". Phys. Rev. Lett. PRL 106, 213901 https://doi.org/10.1103/PhysRev Lett.106.213901.

Longhi, S. 2010. "PT-symmetric laser absorber". Phys. Rev. A-82, 031801(R). https://doi.org/10.1103/PhysRev A.82.031801.

Novitsky, D., Karabchevsky, A., Lavrinenko, A. V., Shalin, A. S., Novitsky, A. 2018. "PT symmetry breaking in multilayers with resonant loss and gain locks light propagation direction". Physical Review B 98(12):125102. DOI: 10.1103.

Novitsky, D., Novitsky, A., Shalin, A.S. "PT-symmetric multilayer systems: homogenization and beam propagation". Conference: 2019 Thirteenth International Congress on Artificial Materials for Novel Wave Phenomena (Metamaterials), Agosto 2019. DOI: 10.1109/MetaMaterials.2019.8900885

Padrón-Godínez, A., Prieto Meléndez, R., Calva Olmos, G., Treviño-Palacios, C. G. 2019. "Sistemas Rectificadores de Señales mediante Diodos Ópticos y Electrónicos". SOMI XXXIV, Congreso de instrumentación, Morelia, Michoacán-México. Volumen: No. 1, Año 6, ISSN 2395-8499.

Poladian, L. 1996. "Resonance mode expansions and exact solutions for nonuniform gratings," *Phys. Rev. E.* 54, 2963.

Ramezani, H., Kottos, T. 2010. "Unidirectional nonlinear PT-symmetric optical structures". Phys. Rev. A-82, 043803. https://doi.org/10.1103/PhysRevA.82.043803.

Rodríguez-de Marcos, L. V., Larruquert, J. I., Méndez Aznárez, J. A. 2016. "Self-consistentopticalconstants of SiO_2 and Ta_2O_5 films", Opt. Mater. Express 6, 3622-3637 (Numerical data kindly provided by Juan Larruquert).

Schilling, D. L., Belove, C. 1989. "Electronic Circuits". 3rd ed. McGraw Hill.

Shramkova, O. V., Tsironis, G. P. 2016. "Scattering properties ofPT- symmetric layered periodic structures". *J. Opt.* 105101 (9pp), DOI:10.1088/2040-8978/18/10/105101.

Steck, A. D. 2006. "Classical and Modern Optics". University of Oregon.

Yang, E., Lu, Y., Wang, Y., Dai, Y., Wang, P. 2016. "Unidirectional reflection less phenomenon in periodic ternary layered material". OSA. DOI:10.1364/OE.24. 014311 |OPTICS EXPRESS 14311.

Yuan, L., Lu, Y. Y., 2019. "Unidirectional reflectionless transmission for two-dimensional PT-symmetric periodic structures".Phys. Rev. A., 100.053805. DOI: 10.1103.

****